The Impact of Hybridization on Upper First Molar Shape in Robust Capuchins (*Sapajus nigritus x S. libidinosus*)

Emma Ayres Kozitzky[1*]

[1] New York University

ABSTRACT To better understand the impact of hybridization on development and morphology, I analyze an understudied phenotype in hybrid morphology research: tooth shape. I apply a 2D geometric morphometric approach to compare variation in first upper molar cusp tip positions and crown outline shape among 31 crested capuchins (*Sapajus nigritus*), 37 bearded capuchins (*S. libidinosus*), and 44 hybrids (*S. nigritus* x *S. libidinosus*). A principal components analysis shows that group membership accounts for a significantly greater proportion of variance along the first major axis of M^1 shape variation than does allometry. While most hybrids have *S. nigritus*-like M^1s, several possess a transgressive M^1 shape not observed in either parental species. Procrustes distances are greater in hybrids compared to the parental capuchins, and two-block partial least squares analyses show that hybrids exhibit weaker integration between cusp tip positions and crown outline shape. These results demonstrate that hybridization generates novel M^1 shapes and support the hypothesis that destabilized development results in elevated phenotypic variance in hybrids. Further studies of dental shape in hybrid primates will generate important data for on-going efforts to detect potential hybrids in the hominin fossil record and to understand the evolutionary outcomes of anthropogenic hybridization.

Hybridization, once viewed as rare and universally detrimental (Dobzhansky, 1940; Mayr, 1963), is increasingly viewed as a frequent and innovative evolutionary phenomenon (Ackermann et al., 2019; Arnold, 1997; Taylor & Larson, 2019). Adaptive hybridization and fertile hybrid populations have been observed in a wide array of animals and plants, such as Galápagos finches (Grant & Grant, 2020), toads (C. Chen & Pfennig, 2020), butterflies (Jiggins et al., 2008), and poplar trees (Chhatre et al., 2018). There is an especially rich body of literature on ancient and contemporary primate hybridization. Genetic analyses have demonstrated that hybridization events occurred in many primate lineages during their course of evolution (de Manuel et al., 2016; Fan et al., 2018; Kuhlwilm et al., 2019; Svardal et al., 2017; Tung & Barreiro, 2017; Zichello, 2018), including hominins (Browning et al., 2018; L. Chen et al., 2020; Durvasula & Sankararaman, 2020; Green et al., 2010; Huerta-Sánchez et al., 2014; Reich et al., 2011; Slon et al., 2018). A growing number of primate taxa are proposed to have hybrid origins (Burrell et al., 2009; Detwiler, 2019; Rogers et al., 2019; Roos et al., 2019; Thinh et al., 2010; Tosi et al., 2000; Wang et al., 2015). Hybridization continues to shape genetic and phenotypic variation in present-day primate populations in both natural and anthropogenic contexts (Alberts & Altmann, 2001; Bergman et al., 2008; E. L. Bynum et al., 1997; Cortés-Ortiz et al., 2007; Gligor et al., 2009; Jolly et al., 2011; Malukiewicz et al., 2015; Mather, 1992).

While genetic analysis has been crucial for exploring primate hybridization, there is a growing interest in understanding the impact of hybridization on morphology. Studies of hybrid primate morphology offer unique insight into the effect of

*Correspondence to:
Emma Ayres Kozitzky
Department of Anthropology
Center for the Study of Human Origins
New York University
New York, NY 10003
eak475@nyu.edu

rapid genetic recombination on phenotypic development and variation. Many studies have evaluated soft tissue phenotypes in contemporary hybrid populations using traits that are easy to observe in the field and can be measured non-invasively, such as pelage color and distribution, head shape, and tail carriage (Alberts & Altmann, 2001; N. Bynum, 2002; Kelaita & Cortés-Ortiz, 2013; Phillips-Conroy & Jolly, 1986). Researchers have also studied the relationship between hybrid ancestry and hard tissue phenotype, such as skeletodental size, shape, and non-metric trait variation (Ackermann et al., 2006; Ackermann & Bishop, 2010; Boel, 2016; Cheverud et al., 1993; Eichel & Ackermann, 2016; Ito et al., 2015; Kohn et al., 2001; Phillips-Conroy, 1978). The proximate aims of hybrid morphology research are to elucidate how hybrid morphology quantitatively and qualitatively differs from parental morphology and if different kinds of hybrids share diagnosable traits indicative of their hybrid ancestry (Ackermann, 2010; Ackermann et al., 2019).

The data derived from hybrid morphology research has important broader implications for primate conservation and paleoanthropology. Primate conservation biologists observe that the frequency of hybridization will likely increase as primate habitats are disturbed or destroyed by anthropogenic interference (Detwiler et al., 2005; Malukiewicz, 2019; Thompson et al., 2018). Rare, endangered primates may reproduce with more common heterospecifics if conspecific mates are difficult to find. Extensive admixture between divergent taxa may result in loss of genetic and phenotypic diversity and ultimately fuse two lineages (Seehausen et al., 2008), or it may generate novel diversity and prevent inbreeding depression (Arnold & Meyer, 2006). By studying the variation in hybrid phenotypes, conservation biologists may be able to understand if the outcomes of anthropogenic hybridization are harmful, neutral, or adaptive for endangered primate populations.

Paleoanthropologists acknowledge that hybrid hominins are likely present in the fossil record. Fossil evidence demonstrates that multiple hominin taxa cohabited Africa and Eurasia throughout the Pliocene and Pleistocene and could have hybridized where their ranges overlapped (Détroit et al., 2019; Grün et al., 2020; Herries et al., 2020; Spoor et al., 2015). The genetic evidence for hybridization events throughout hominin evolution is substantial (Durvasula & Sankararaman, 2020; Jacobs et al., 2019; Sankararaman et al., 2016; Skov et al., 2020; Villanea & Schraiber, 2019). The hybrid

ancestry of several fossilized hominin individuals has been confirmed by ancient DNA analyses (Fu et al., 2015; Slon et al., 2018). However, ancient DNA preservation is rare in most of the hominin fossil record, so analyses of hard tissue phenotypes in extant hybrid primates can be used to assess the feasibility of using morphological indicators to identify hybrid hominin fossils (Ackermann et al., 2019). The identification of hybrid hominin fossils remains an outstanding issue for reconstructing hominin phylogenetic relationships, as most the commonly used phylogenetic frameworks assume evolutionary relationships are hierarchical rather than reticulate (Holliday, 2003).

Quantitative genetic theory states that in first-generation (F1) hybrids, phenotypic trait measurements controlled by additive genetic variation will be the midparental value (MPV), or the averaged parental measurements (Falconer & Mackay, 1997). Tests of this theory indicate that while some F1 hybrid primate phenotypes exhibit the expected MPV (Hamada et al., 2012), other traits in the same population may deviate from the expected phenotype (Ackermann et al., 2006; Cheverud et al., 1993; Eichel & Ackermann, 2016). Positive deviations from the MPV in F1 populations is referred to as heterosis, or hybrid vigor, while negative deviations are evidence of dysgenesis, or hybrid breakdown. Later-generation hybrids with higher genetic input from one parental taxon are expected to be more phenotypically like that parent, but some hybrids resemble one parent more than the other, regardless of parental genetic contribution (Boel et al., 2019; Ito et al., 2015). First- and later-generation hybrid populations sometimes exhibit transgressive phenotypes not observed in either parental population, such as extreme trait size, novel combinations of parental traits, or the presence of non-metric craniodental anomalies (Ackermann et al., 2014; Ackermann & Bishop, 2010; Jolly et al., 1997). Research on hybrid morphology in primates has documented a complex array of phenotypic outcomes that vary within and among hybrid populations (Alberts & Altmann, 2001). Importantly, these outcomes are not universally maladaptive (Charpentier et al., 2012) and may help hybrid populations occupy ecological niches unavailable to either parental population, thereby resulting in novel evolutionary lineages (Arnold, 1997; Zinner et al., 2011).

The high morphological variability observed within and among hybrid populations is thought to be the result of destabilized development (Clarke, 1993). The uniquely adapted developmen-

tal regimes of two distinct parental taxa are unlikely to merge seamlessly in offspring and could result in perturbations during hybrid morphogenesis. This is supported by the observation that deviations from predicted F1 midparental phenotypes tend to be more pronounced with increasing genetic distance between parental populations (Bernardes et al., 2017; Z. J. Chen, 2013; Stelkens & Seehausen, 2009). Researchers have tested the hypothesis that hybrids experience destabilized development using tests of morphological integration and fluctuating asymmetry (Alibert et al., 1994; Jackson, 1973; Klingenberg, 2003; Klingenberg & McIntyre, 1998). Tightly integrated trait complexes and highly symmetric bilateral trait measurements are hypothesized to reflect stable, canalized development. So, if hybridization results in developmental destabilization, hybrids are expected to exhibit weaker trait integration and greater fluctuating asymmetry between bilateral traits than parental taxa. Some hybrids do meet these expectations (Ackermann et al., 2014; Leary et al., 1985; Neff & Smith, 1979), but others do not differ from observed levels of parental trait integration or fluctuating asymmetry (Jackson, 1973; Pallares et al., 2016). In some cases, hybrid samples exhibit stronger trait integration and bilateral trait symmetry than parents, indicating that hybrid development is more stable than parental development (Alibert et al., 1994; Boel et al., 2019; Debat et al., 2000).

Despite growing interest in primate hybrid morphology, the relationships among hybrid ancestry, development, and phenotype remain unclear and difficult to predict. However, one of the most potentially informative anatomical regions for this research has also been one of the most understudied: the dentition. Several lines of evidence suggest that in-depth analyses of dental phenotypic variation will produce valuable data for hybrid morphology research. Anomalous dental non-metric traits are observed at high frequencies in some hybrid populations, such as supernumerary teeth, crown rotation and/or malformation, and dental crowding (Ackermann et al., 2010, 2014; Ackermann & Bishop, 2010; Goodwin, 1998; Heide-Jorgensen & Reeves, 1993). Intergeneric hybrids of *Theropithecus gelada* and *Papio hamadryas* ("geboon") exhibit combinations of parental traits in their dentitions, such as *T. gelada*-like enamel crenulation on *P. hamadryas*-like low-crowned molars, resulting in novel dental phenotypes (Jolly et al., 1997). Most of the geboon hybrids also exhibited maxillary cheektooth dimensions that exceeded

the parental means. However, hybrids of more closely related baboon species *P. hamadryas* and *P. anubis* were not easily differentiable from parental species based on both metric and non-metric dental traits (Phillips-Conroy, 1978). Similarly, dental non-metric trait expression did not discriminate between closely related *Macaca fuscata*, *M. cyclopis*, and their hybrids (Boel et al., 2019). Further analyses of dental size, shape, and non-metric trait expression in extant primate hybrids would elucidate if hybrid primates exhibit shared patterns of dental trait variation.

Dental phenotypic analyses of hybrids also could help to understand if deviations from typical parental development generate the high variability observed in hybrid populations. Mammalian dental development is well-studied, and models of dental development have been tested in both extinct and extant primates (Evans et al., 2016; Hlusko et al., 2016; Jernvall & Jung, 2000; Ortiz et al., 2018; Paul et al., 2017). The iterative nature of dental development results in predictable patterns of dental trait integration both within the same tooth crown and among metameres. The patterning cascade model claims that the duration of tooth germ growth and the spatiotemporal distribution and strength of embryonic signaling centers within the germ constrain possible cusp configurations and crown size in the fully formed tooth (Jernvall, 2000). So, differences between parental and hybrid cusp configurations and accessory cusp expression likely reflect deviations in underlying patterning cascade pathways. Similarly, the inhibitory cascade model states that mammalian mandibular molar number and relative size are dictated by embryonic signaling strength and duration of odontogenesis, so differences between hybrid and parental molar size relationships and molar number likely reflect differences in this developmental pathway as well (Kavanagh et al., 2007). Indeed, in a hybrid baboon population, supernumerary mandibular molars are positively correlated with increased molar row length, which suggests that dental development is prolonged in the hybrids compared to parents (Ackermann et al., 2014).

Data derived from studies of hybrid dentitions is especially useful for conservation biologists and paleoanthropologists. Results derived from studies of hybrid skulls and postcrania are not easily applied in living primate populations, but the teeth of primates in hybrid zones can be evaluated, photographed, or molded and cast during trapping expeditions (Kelaita & Cortés-Ortiz, 2013; Phillips-Conroy, 1978). While skeletal data is certainly use-

ful for paleoanthropologists interested in determining the feasibility of identifying hybrid ancestry using fossil morphology, teeth tend to be better preserved and comprise most of the hominin fossil record (Bailey, 2002; Gómez-Robles et al., 2007; Martinón-Torres et al., 2012; Wood & Abbott, 1983).

The genus *Sapajus* is an excellent study taxon for hybridization research. The robust capuchin clade underwent rapid radiation and expansion during the Pleistocene, and species often interbreed where their ranges meet (Lima et al., 2018; Lynch Alfaro, Boubli, et al., 2012), making them an appropriate analog for understanding hominin hybridization. A sample of hybrids of *Sapajus nigritus* and *S. libidinosus* are housed at the Smithsonian National Museum of Natural History (NMNH). *Sapajus nigritus* and *S. libidinosus* shared a common ancestor approximately 2.6 Ma and belong to different clades within the genus, the former belonging to a more ancient clade endemic to the Atlantic Forest of Brazil, and the latter belonging to a recently evolved clade adapted to Brazilian dry shrublands (Lima et al., 2018; Wright et al., 2015). Both species are listed as 'near threatened' by the IUCN Red List of Threatened Species and both are known to occupy habitats disturbed by agricultural practices (Melo, Alfaro, et al., 2015; Melo, Fialho, et al., 2015). It is possible that anthropogenic hybridization could result in the loss of genetic and phenotypic diversity among robust capuchin species (Lynch Alfaro et al., 2014; Martins et al., 2017). A morphological analysis of hybrid robust capuchins would establish if phenotypic diversity is impacted by hybridization.

Here, I apply 2D geometric morphometric (2DGM) techniques to study variation in first upper molar (M^1) crown outline shape and cusp tip configuration among *Sapajus nigritus*, *S. libidinosus*, and their hybrids. Dental shape has been used to study population affinity and to characterize extinct and extant primate taxa (Bailey et al., 2016; Gamarra et al., 2016; Gómez-Robles et al., 2007, 2015; Rizk et al., 2013), including robust capuchins (Delgado et al., 2015), but has not yet been used to study patterns of morphological variation among hybrids and their parental taxa. The primary aims of this study are to explore variation and the factors driving variation in M^1 morphology in hybrids compared to *S. nigritus* and *S. libidinosus*; to determine if M^1 morphology can discriminate between hybrids and parental taxa; and to evaluate if hybrids exhibit evidence of destabilized dental development compared to parental taxa. Based on previous hybrid morphology research, I tested the following predictions:

1) M^1 shape is statistically distinct among *S. nigritus*, *S. libidinosus*, and their hybrids.
2) The mean shape of hybrid M^1s is the midparental value (the mean shape of the combined parental sample).
3) There is more variability in M^1 shape within the hybrid sample than within either parental sample.
4) Hybrids exhibit weaker covariation between cusp tip configuration and crown outline shape than parental taxa.

Materials and Methods

My sample includes *Sapajus nigritus* (*n* = 31), *S. libidinosus* (*n* = 37), and a hybrid sample of *S. nigritus* x *S. libidinosus* (*n* = 44). The dental sample comprises 112 right M^1s (Table 1). Only specimens with unworn or minimally worn M^1s were included.

Table 1. Number of M^1s included in this study.

	Female	Male	Total
Sapajus nigritus	16	15	31
S. nigritus x *S. libidinosus*	21	23	44
S. libidinosus	21	16	37
Total	58	54	112

I used a Nikon D500 DSLR digital camera fitted with a macro lens and attached to a copy stand to photograph M^1 occlusal surfaces. I positioned the M^1 cementoenamel junction (CEJ) parallel to the lens and included a scale placed at the same level as the occlusal plane (Bailey, 2004; Gómez-Robles et al., 2007). While directly referencing the specimen, I marked each of the four main M^1 cusp tips (the paracone, protocone, metacone, and hypocone) on the digital images using the GNU Image Manipulation Program version 2.10.12 (The GIMP Development Team, 2019). If a specimen exhibited slight wear, I marked the cusp tip in the center of the wear facet.

I uploaded the photographs to TpsDig2 version 2.31 to digitize a series of 2D landmarks (points of biological homology among specimens) and semi-landmarks (non-homologous points of morphological interest; Bookstein, 1997). Landmarks 1 through 4 were placed on the tips of the paracone, protocone, metacone, and hypocone (Figure 1). These landmarks capture variation in the position

of the main cusps relative to each other and relative to the crown outline. In order to examine variation in the shape of M[1] crown outlines, I placed 30 semilandmarks around the perimeter of the occlusal surface, starting at the point of maximum curvature where the buccal and mesial margins intersect. I drew a closed curve around the crown outline, and then appended 29 additional equidistant semilandmarks to the curve (see Figure 1). Finally, I exported all landmark and semilandmark coordinates as a .tps file to RStudio version 1.2.5033 for analysis.
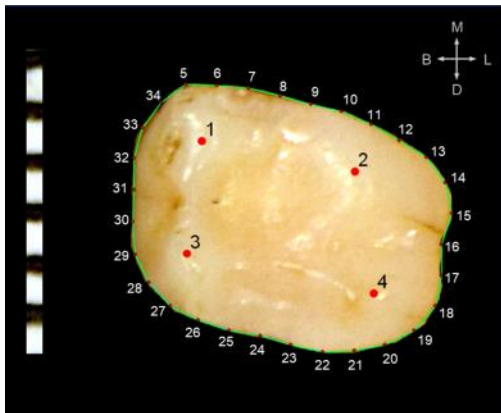

Figure 1. The landmark (1-4) and semilandmark (5-34) configuration used to analyze variation in M[1] cusp tip position and crown outline shape. M: mesial; D: distal; B: buccal; L: lingual.

All geometric morphometric analyses were performed using the R package geomorph (Adams et al., 2020). First, I defined semilandmarks 5 through 34 as sliding semilandmarks. Sliding semilandmarks can move along the crown outline between neighboring semilandmarks to optimize their position with respect to the average shape of the entire sample. This process removes random variation from the coordinate data introduced by the initial arbitrary placement of semilandmarks around the crown margin and converts semilandmarks 5 through 34 to homologous points statistically comparable to landmarks 1 through 4 (Gunz & Mitteroecker, 2013). Next, I performed a generalized Procrustes analysis (GPA) on the landmark and sliding semilandmark coordinates to remove the effects of specimen size, orientation, and position, leaving only variation related to shape. The GPA superimposes specimens by translating, scaling, and rotating the coordinates to generate an average shape, or consensus configuration, for the entire sample (Bookstein, 1997;

Zelditch et al., 2012). I used the results of the GPA for all subsequent analyses.

To explore and compare major axes of M[1] shape variation among *S. nigritus*, *S. libidinosus*, and their hybrids, I conducted a principal components analysis (PCA). To visualize variation in shape space, I plotted PC 1 against PC 2 and PC 2 against PC 3. I included 95% confidence ellipses for each taxon to illustrate within-taxon variability. Then, to test the effect of allometry on M[1] shape, I constructed twelve linear models using results from the PCA (Table 2a). Each model tested the association between scores on PCs 1, 2, and 3 with taxonomic designation, logarithm-transformed centroid size, or a combination of both variables. The best-fitting model for PCs 1, 2, and 3 were selected using the function for Akaike's information criterion (AIC) in the R package bbmle (Bolker et al., 2020).

I used warp grids representing the mean shape for each taxon to visually evaluate if and how M[1] shape varies among groups. To statistically evaluate the extent to which M[1] shape is morphologically distinct among these groups by maximizing intergroup differences, I extracted the first ten PCs derived from the PCA (encompassing the majority of shape variation within the sample) for a discriminate function analysis (DFA). Then I used the results from the DFA for a cross-validated assignment test.

I measured within- and between-group variance using pairwise Procrustes distances (the Euclidean distance between two sets of shape coordinates; Spoor et al., 2015). A Procrustes distance equal to zero represents a pair of individuals with identical M[1] shape, while increasing distance reflects increasing dissimilarity in shape. I evaluated statistical differences in Procrustes distances among taxa using pairwise *t*-tests using Bonferroni correction for multiple comparisons.

I performed a two-block partial least squares analysis (2B PLS) to evaluate the level of covariation between the position of cusp tips (block 1: landmarks 1 through 4) and the shape of the crown outline (block 2: sliding semilandmarks 5 through 34), and implemented a permutation procedure (*n* = 1,000 permutations) to test the *r*-PLS correlation coefficients generated by the 2B PLS for statistical significance. Because calculation of the *r*-PLS statistic is dependent on sample size, I employed a standardized *z*-score converted to pairwise effect sizes to compare the strength of integration among groups (Adams & Collyer, 2016). Large pairwise effect sizes indicate that the level of morphological integration differs between the two samples.

Results

Mean M^1 shape in parental and hybrid taxa

The mean shapes for *S. nigritus*, *S. libidinosus*, and the hybrids compared to the pooled-sample consensus configuration are shown in Figures 2a, 2b, and 2c, respectively. Differences in mean shape are magnified by a factor of three to assist in visual interpretation. The average crown outline shape in *S. nigritus* is rhomboid, while that of *S. libidinosus* is more ovoid. The average crown outline in the hybrid sample is more mesiobuccally skewed than either parental taxon and has a waisted lingual margin. The two parental taxa exhibit similar inter-cusp distances relative to the crown outline, but the mean *S. nigritus* paracone, metacone and hypocone (landmarks 1, 3, and 4, see Figure 1) are buccally displaced compared to the consensus cusp tips. The average hybrid protocone, paracone, and metacone (landmarks 1 through 3, see Figure 1) are slightly mesially displaced compared to the consensus configuration. The average hybrid M^1 shape differs from the expected midparental shape. The midparental M^1 crown outline does not have the waisted lingual margin that is present in the hybrid mean outline, and the hybrid protocone, paracone, and metacone are mesially displaced compared to the expected midparental M^1 cusp configuration.
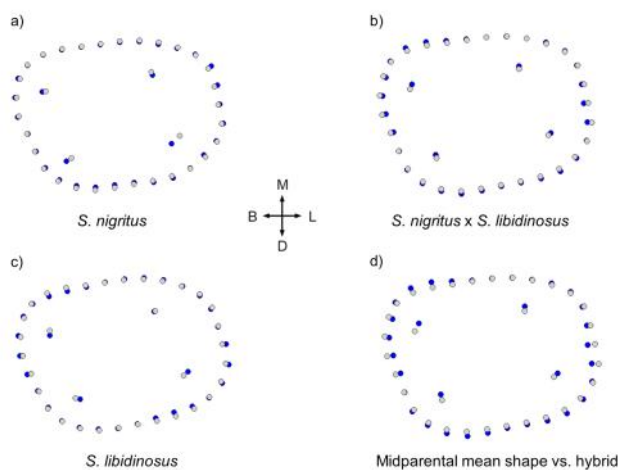

Figure 2. Pooled sample consensus M^1 shape (gray) compared to mean M^1 shape (blue) among (a) *S. nigritus,* (b) *hybrids*, and (c) *S. libidinosus*. Figure 2d illustrates the mean parental M^1 shape (*S. nigritus* and *S. libidinosus* combined, light gray) and the transformation of the mean parental M^1 shape into the mean hybrid shape (blue). All comparisons are magnified by a factor of 3 to aid in visual interpretation. M: mesial; D: distal; B: buccal; L: lingual.

Principal components analysis

The first three PCs account for approximately half (48.1%) of the variation in M^1 shape among *S. nigritus*, *S. libidinosus*, and *S. nigritus* x *S. libidinosus*. Principal component 1 explains 20.8% of shape variation, while PC 2 explains 16.6% (Figure 3a). The warp grids representing M^1 shape at extreme ends of variation along each PC illustrate that M^1s with low PC 1 scores have a mesiobuccally skewed rhomboid crown outline which tapers distally and a waisted lingual margin. The cusp tips are displaced towards the buccal margin. First molars with high PC 1 scores have squared, symmetrical outlines and roughly equidistant cusp tips. Along PC 2, M^1s with low scores have mesiobuccally skewed rhomboid outlines with cusp tips displaced towards the buccal margin, while M^1s with high scores have more symmetrical crown outlines, increased buccolingual distance between the two mesial cusps and between the two distal cusps, and lingual displacement of the lingual cusps. There is substantial overlap among the three taxa, but hybrids tend to have low PC 1 scores and high PC 2 scores, while the parental taxa tend to have high PC 1 scores and low PC 2 scores. The 95% confidence ellipse for hybrids is much broader than those of the parental taxa, reflecting greater variation in shape space.

Principal component 3 accounts for 11.2% of M^1 shape variation (Figure 3b). First molars with low PC 3 scores have symmetrical and ovoid crown outlines and a rhomboid cusp tip configuration. High scores on PC 3 correspond to M^1s with mesiobuccally skewed, rhomboid crown outlines with a waisted lingual margin, wide intercusp spacing, and all cusp tips displaced towards the periphery. There is very little separation among taxa in PC 2 vs. PC 3 shape space. The range of variation among *S. nigritus* individuals is almost entirely subsumed within the range of the hybrids. *S. libidinosus* tends to cluster on the low end of PC 2 away from *S. nigritus* and the hybrids. Based on shape and size of the 95% confidence ellipses projected onto tangent space for each taxon, the hybrids exhibit the highest variation in M^1 shape along PCs 2 and 3.

Regression analysis and allometry

The regression analysis demonstrated that taxonomic designation explains more variation in PC 1 scores than does M^1 size (Tables 2a and 2b). Approximately 20% ($p < 0.001$) of variation in PC 1 scores is explained by taxonomic designation. A post-hoc pairwise *t*-test using Bonferroni adjustment for multiple comparisons showed that hybrids had significantly lower scores on PC 1 than
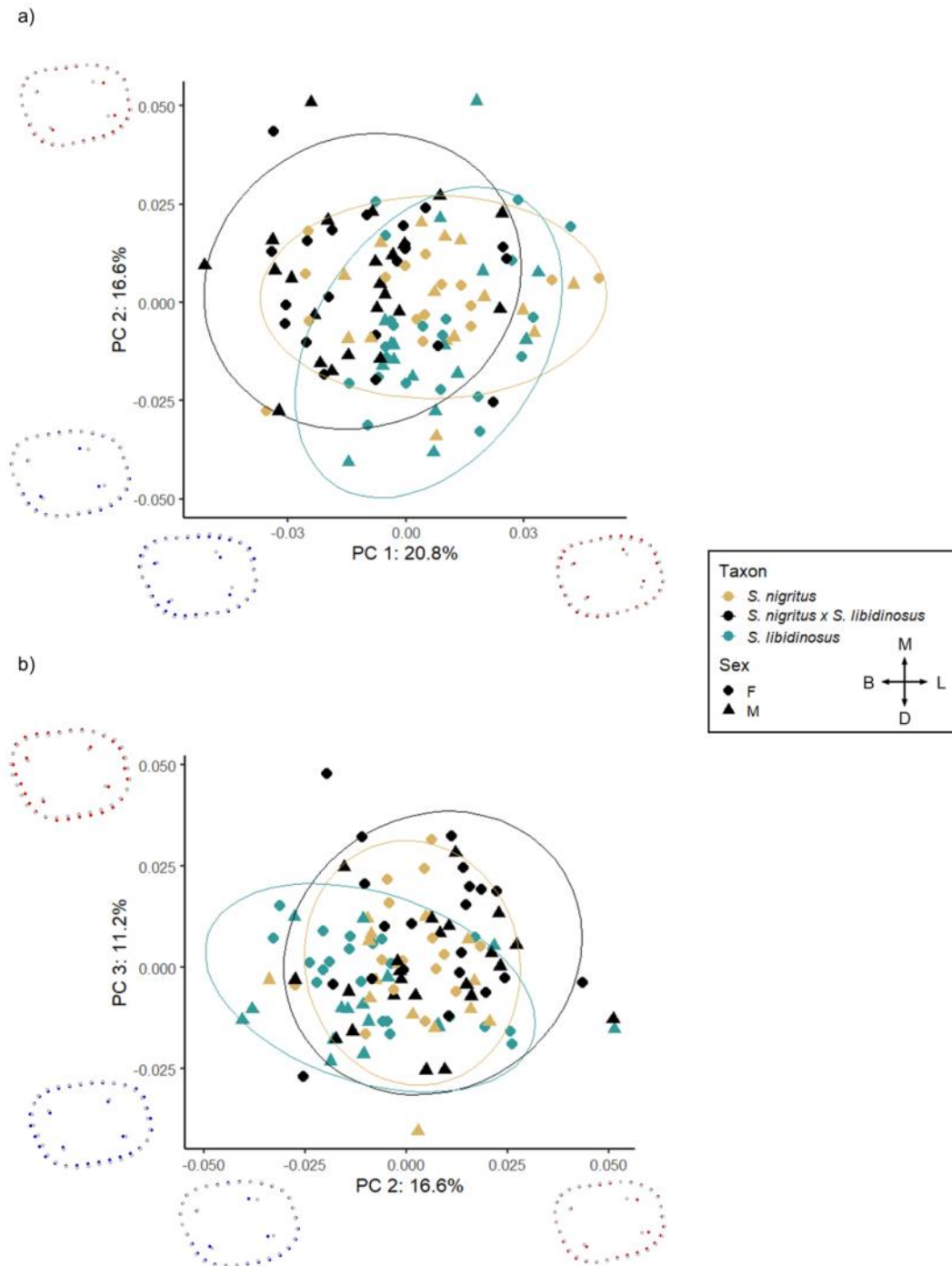
a)

b)

Figure 3. Scatter plots of (a) PC 1 against PC 2 scores, and (b) PC 2 scores against PC 3 scores derived from the PCA of M¹ shape. The warp grids illustrate the transformation of the consensus configuration (gray) into the shape of M¹s with the lowest (blue) and highest (red) scores along PCs 1 and 2. Ellipses represent 95% confidence intervals for each group. Note that, while there is considerable overlap among the groups, the hybrids tend to exhibit lower PC 1 and higher PC 2 scores than the parental taxa, corresponding to M¹s with skewed crown outlines, a waisted lingual margin, and wider intercusp distances. M: mesial; D: distal; B: buccal; L: lingual.

Table 2. Results of the regression analysis assessing the effect of taxonomic designation and allometry on variation in the first three principal component (PC) scores.

a)

Model #	Model Terms	R²	*p*-value
1	PC 1 ~ log(centroid size)	0.02	0.20
2	**PC 1 ~ taxon**	**0.20**	**<0.001**
3	PC 1 ~ taxon + log(centroid size)	0.22	<0.001
4	PC 1 ~ taxon * log(centroid size)	0.22	<0.001
5	PC 2 ~ log(centroid size)	0.06	0.008
6	PC 2 ~ taxon	0.11	0.002
7	**PC 2 ~ taxon + log(centroid size)**	**0.17**	**<0.001**
8	PC 2 ~ taxon * log(centroid size)	0.18	<0.001
9	PC 3 ~ log(centroid size)	0.01	0.29
10	**PC 3 ~ taxon**	**0.07**	**0.02**
11	PC 3 ~ taxon + log(centroid size)	0.09	0.02
12	PC 3 ~ taxon * log(centroid size)	0.09	0.08

The best-fitting model for each PC is in bold.

b)

PC	Model #	AIC	dAIC	df	Weight
1	**2**	**-567.3**	**0.0**	**4**	**0.526**
	3	-566.7	0.6	5	0.383
	4	-563.8	3.5	7	0.091
	1	-546.3	21.1	3	<0.001
2	**7**	**-586.3**	**0.0**	**5**	**0.653**
	8	-584.6	1.7	7	0.284
	6	-581.3	5.0	4	0.054
	5	-577.4	8.9	3	0.007
3	**10**	**-619.6**	**0.0**	**4**	**0.478**
	11	-619.3	0.3	5	0.416
	12	-615.6	4.0	7	0.066
	9	-614.6	5.0	3	0.040

The best-fitting model for each PC is in bold.

both *S. nigritus* and *S. libidinosus* (p = 0.003 and $p <$ 0.001, respectively), but no significant difference in PC 1 scores between *S. nigritus* and *S. libidinosus* (p = 0.99; Figure 4a). More complex models testing the effect of taxonomic designation on the relationship between PC 1 scores and M[1] size were non-significant. Change in M[1] shape along the main axis of variation is not driven by size alone. However, the next-best-fitting model according to AIC suggested that the average PC 1 score estimated from M[1] size varies by taxon.

A more complex model is required to explain variation in PC 2 scores. First molar size and taxonomic designation only explain 6% (p = 0.008) and 11% (p = 0.002) of variation in PC 2 scores, respectively, and a comparison of the two models indicates that PC 2 ~ taxon is a better fit than PC 2 ~ log(centroid size) (F = 5.93, p = 0.02). A post-hoc comparison of differences in PC 2 scores by taxon indicates that *S. libidinosus* has significantly lower PC 2 scores than the hybrids (p = 0.001; Figure 4b); all other pairwise comparisons are non-significant. A multivariate model combining the effect of taxonomic designation and M[1] centroid size explains 17% (p < 0.001) of variation in PC 2 scores and is a significantly better fit than PC 2 ~ taxon. There is no significant increase in explanatory power with the addition of an interaction term describing change in the slope of the relationship between M[1] shape and size among taxa (F = 1.12, p = 0.33). So, variation in shape along PC 2 is partly driven by size, but the average PC 2 score estimated from M[1] size differs by taxon.

As with PC 1, taxonomic designation explains the most variation in PC 3 scores rather than M[1] size. However, the amount of variation in PC 3 scores explained by taxonomic designation is small (R[2] = 0.07, p = 0.02), and a post-hoc comparison average PC 3 scores by taxon indicates that the only significant difference among taxa is between *S. libidinosus* and the hybrids (p =0.016, Figure 4c). Comparisons with more complex models accounting for different size/shape relationships by taxon

do not add significant explanatory power.

Discriminant function analysis
Results for the discriminant function analysis are illustrated in Figure 5. The DFA maximized differences in between-group variation, but there is little separation among parental species and their hybrids along linear discriminant functions (LDs) 1 and 2. Along LD 2, there is some separation between *S. libidinosus,* which clusters at the positive end, and *S. nigritus* and hybrids, which both cluster toward the negative end. Most of the hybrids have negative loadings on LD 1 and LD 2.

The results of the cross-validated assignment test are presented in Table 3. The percentage of individuals correctly classified to their *a priori* assigned taxon ranges from only slightly better than chance in *S. nigritus* (61.3%) to moderate in *S. libidinosus* (73.0%). In the hybrid group 70.5% were correctly assigned as such. Both *S. nigritus* and *S. libidinosus* misclassified individuals were more frequently assigned to the hybrid group than to the wrong parental taxon, reflecting higher variation in M[1] shape among hybrids.

Procrustes distances within and among taxa
The mean pairwise Procrustes distances in M[1] shape are listed in Table 4, and frequency distributions of pairwise Procrustes distances within and between taxa are visualized in Figure 6. The average distance for the entire sample is 0.06. Within-taxon shape variability is highest for the hybrids (distance = 0.059) compared to the parental taxa (*S. nigritus* = 0.055, *S. libidinosus* = 0.053). All three taxa have significantly different mean Procrustes distances (p < 0.001). The between-taxa comparisons show a greater degree of similarity between *S. libidinosus* and *S. nigritus* M[1] shape (distance = 0.058) than between each parental taxon and the hybrids, and there is approximately equal distance between the parental taxa and the hybrids (*S. nigritus* vs. hybrids = 0.061, *S. libidinosus* vs. hybrids = 0.062).

Table 3. Results of the cross-validated assignment test. The number of individuals correctly assigned to their a priori designated taxon are in bold.

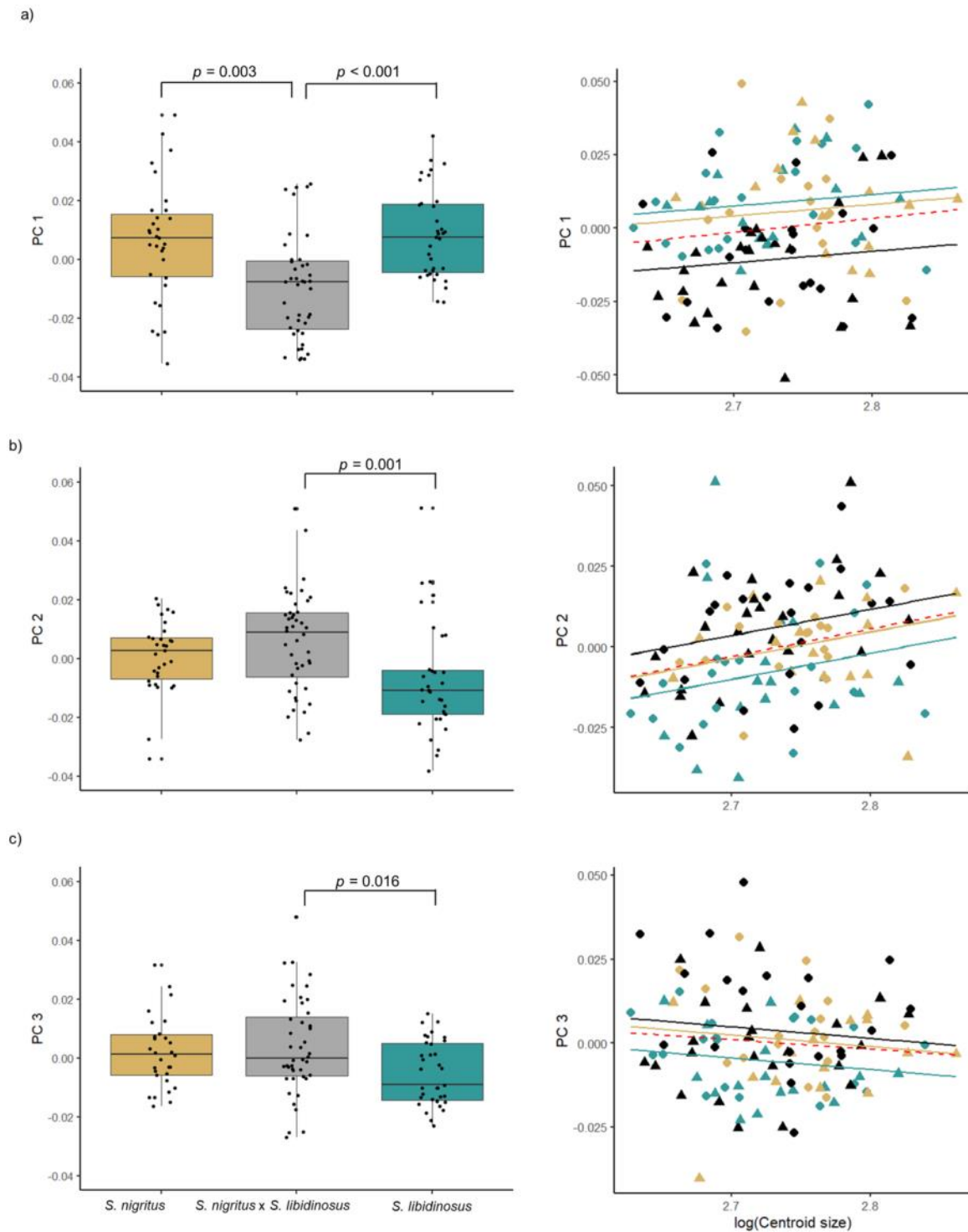|	*S. nigritus*	*S. nigritus* x *S. libidinosus*	*S. libidinosus*	% Correct
S. nigritus	**19**	8	4	61.3
S. nigritus x *S. libidinosus*	5	**31**	8	70.5
S. libidinosus	4	6	**27**	73.0

Figure 4. Box-and-whisker plots and scatterplots of comparing the relationship among taxonomic designation, log-transformed M^1 centroid size, and scores for (a) PC 1, (b) PC 2, and (c) PC 3. The *p*-values for significant differences in PC scores between groups are indicated above the brackets. The red dashed regression line on each scatterplot represents a simple PC score ~ log(centroid size) model. indicates the line of best fit for the pooled sample (PC 2 ~ log(Centroid size)). Based on Akaike's information criterion, the variation in PC 1 and 3 scores is best explained by taxonomic designation (Table 2b), while average PC 2 scores estimated from log(Centroid size) significantly differ among taxa (indicated by separate lines of best fit for each taxon; PC 2 ~ taxon + log(Centroid size)).
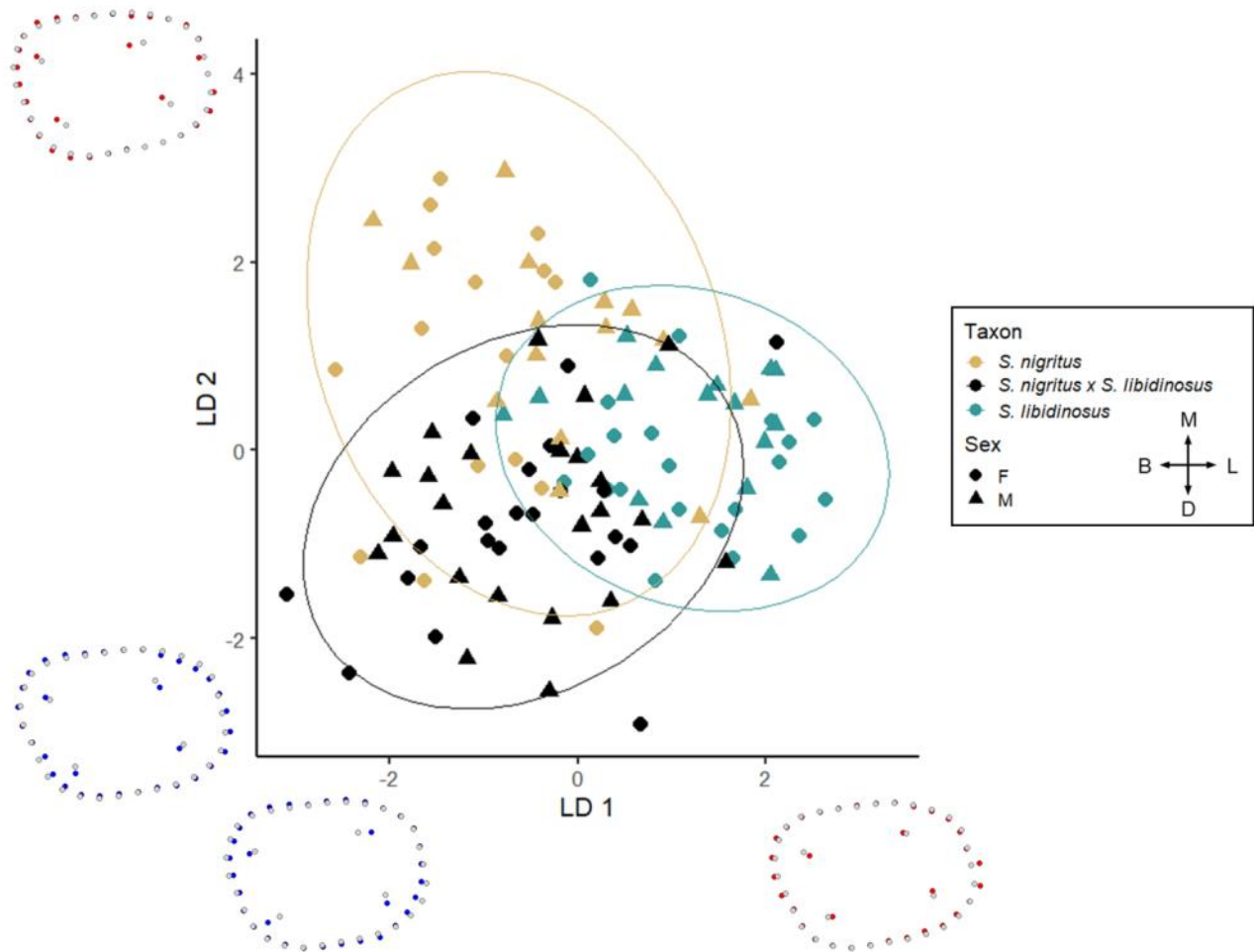
Figure 5. Scatter plot of LDs 1 and 2 derived from the linear discriminant function analysis, in which among-group differences in M^1 shape are maximized. Ellipses represent 95% confidence intervals for each group. First molar shapes along the low end of LDs 1 and 2 are shown in blue, while shapes for M^1 on the high end of LDs 1 and 2 are illustrated in red. M: mesial; D: distal; B: buccal; L: lingual.

Table 4. Mean pairwise Procrustes distances within and between taxa. A Procrustes distance value of 0 means that there is no difference in M^1 shape between two individuals.

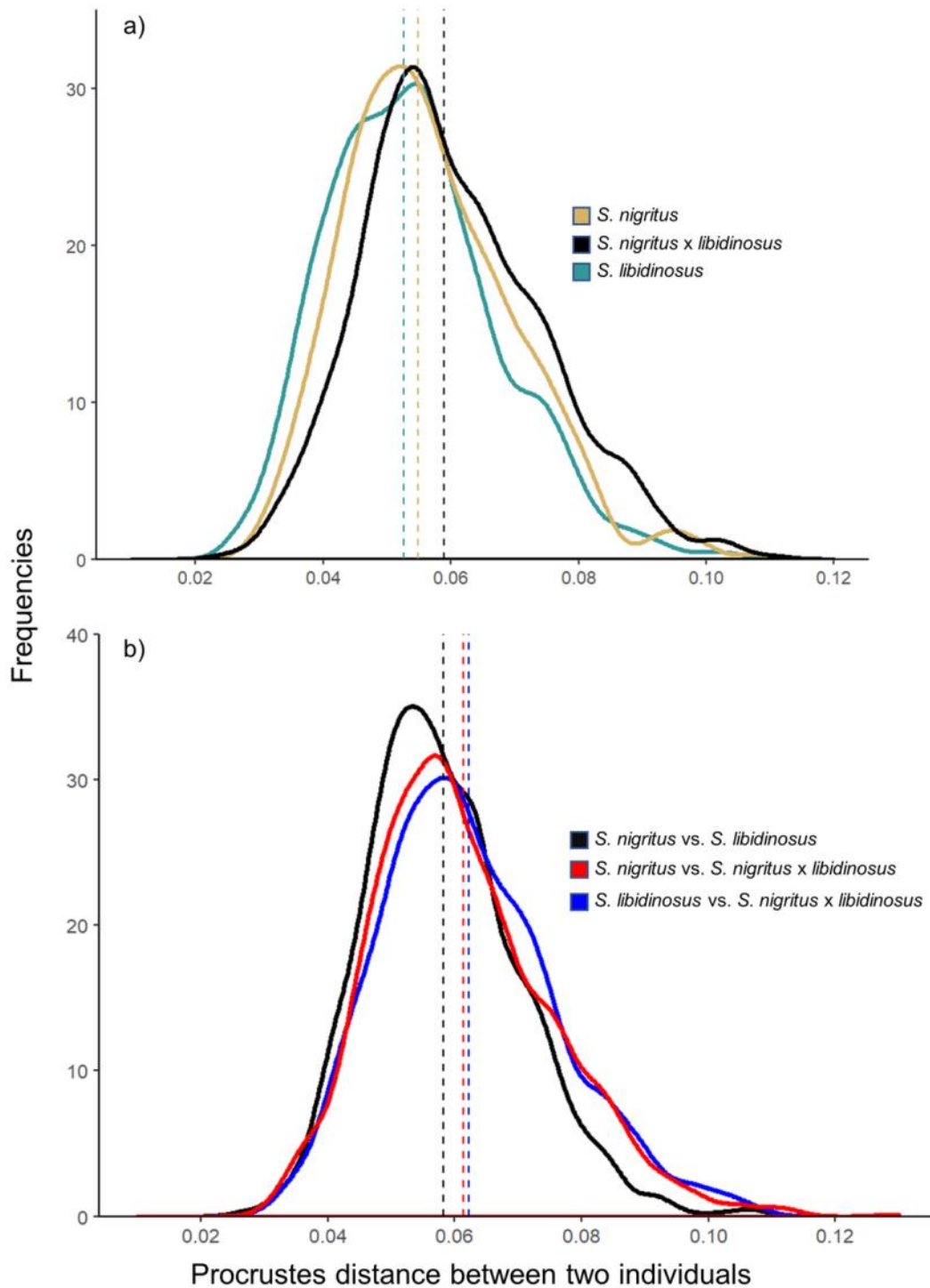|	S. nigritus	S. nigritus x S. libidinosus	S. libidinosus
S. nigritus	0.055		
S. nigritus x S. libidinosus	0.061	0.059	
S. libidinosus	0.058	0.062	0.053

Figure 6. Frequency distributions of (a) within-group, and (b) between-group pairwise Procrustes distances, reflecting degree of similarity in M^1 shape between specimen pairs. Vertical dashed lines represent the mean pairwise Procrustes distance for each group. Note that the hybrids exhibit elevated within-group Procrustes distances, reflecting the higher morphological variability in this group compared to the parental taxa. Also, between-group comparisons between one parental taxon and the hybrids exhibit higher mean Procrustes distances compared to the pairwise distances between parental taxa.

Covariation between cusp tip configuration and crown outline shape

The results of the 2B PLS analysis are summarized in Table 5. There is a strong and statistically significant correlation between cusp tip configuration (block 1) and crown outline shape (block 2) for the combined sample (*r*-PLS = 0.66, *p* = 0. 001). There are differences in covariation between blocks 1 and 2 among the three taxonomic groups. The two parental taxa exhibit high and significant correlations between blocks 1 and 2 (*S. nigritus r*-PLS = 0.76, *p* = 0. 002; *S. libidinosus r*-PLS = 0.75, *p* = 0.001), while the hybrids exhibit weaker correlation between cusp configuration and crown outline shape (*r*-PLS = 0.63, *p* = 0.015). Effect sizes for each sample indicate that the hybrids, compared to the parental taxa, exhibit weaker integration than expected based on its permuted sampling distribution. However, pairwise statistical comparisons indicate that there is no statistically significant difference in the strength of integration among groups (although at *p* = 0.07, the difference in integration between the hybrids and *S. libidinosus* does approach significance; Table 5b).

Discussion

The impact of hybridization on primate hard tissue morphology is difficult to predict. While traits under additive genetic control are expected to exhibit the midparental state in F1 hybrid populations, studies reveal that F1 morphology often deviates from expectations (Ackermann et al., 2006; Ito et al., 2015). Frequently, F1 hybrid trait morphology is polytypic and individuals exhibit novel phenotypes not observed in either parental population (Bergman et al., 2008; Fuzessy et al., 2014; Jolly et al., 1997). Many commonly measured phenotypic traits are not under additive genetic control. Hybridization may affect non-additive trait expression, resulting in heterosis or dysgenesis (Z. J. Chen, 2013). The recombination of two divergently adapted parental genomes in hybrids may disrupt the interaction and expression of non-additive genes that control complex physiological and metabolic networks, including growth and development. This ultimately relaxes the constraints observed in parental developmental pathways and is associated with increased morphological variability in hybrids. Deviations from expected midpa-

Table 5. Results of the two-block partial least squares analysis.

a)

	r-PLS	*p*-value	Effect size
S. nigritus	0.76	0.002	3.01
S. nigritus x S. *libidinosus*	0.63	0.015	2.26
S. libidinosus	0.75	0.001	3.94
Taxa pooled	0.66	0.001	--

The r-PLS value reflects the degree of covariation between configuration of the cusp tips (block 1, landmarks 1 through 4) and the shape of the crown outline (block 2, sliding semilandmarks 5 through 34). Larger effect sizes are associated with stronger observed covariation between cusp tip and crown outline shape than expected based on the permuted sampling distribution.

b)

	S. nigritus	*S. nigritus* x *S. libidinosus*	*S. libidinosus*
S. nigritus	--	0.78	0.47
S. nigritus x *S. libidinosus*	0.79	--	0.07
S. libidinosus	0.60	1.44	--

Matrix of pairwise differences in 2B PLS effect size measuring difference in the strength of integration between samples in the lower triangle with corresponding p-values in the upper triangle.

rental morphology in F1 hybrids are positively associated with increasing parental genetic divergence (Allen et al., 2020; Bernardes et al., 2017; Stelkens & Seehausen, 2009). For example, there are fewer instances of cranial and postcranial trait heterosis in hybrids of recently diverged tamarin subspecies than between crosses of more anciently diverged tamarin subspecies (Cheverud et al., 1993; Kohn et al., 2001). Similarly, non-metric indicators of disrupted skeletodental development tend to be more frequently observed in primates with increasing parental divergence (Ackermann et al., 2014; Boel et al., 2019).

Beyond the first generation, hybrid morphology is expected to more closely resemble that of the parental population into which the hybrids have backcrossed (Falconer & Mackay, 1997). Continuous trait values in the backcrossed offspring of an F1 hybrid and an individual from the parental population are predicted to be the average of the parental value and the MPV. Some novel phenotypes observed in F1 hybrids persist in later-generation hybrids regardless of parental genetic contribution. *Macaca fuscata* x *M. cyclopis* macaques have enlarged, *M. fuscata*-like sinus size even in backcrossed individuals who derive most of their ancestry from *M. cyclopis* (Ito et al., 2015), and transgressive non-metric dental traits are observed in backcrossed *P. cynocephalus* x *P. anubis* individuals (Ackermann et al., 2014). The morphology of individuals in multigenerational hybrid zones depend on a combination of physiological, reproductive, and ecological selective pressures (Charpentier et al., 2008; Fourie et al., 2015; Jolly et al., 2011; Mourthe et al., 2019). These selection pressures structure the distribution of hybrid phenotypes across contact zones. For example, hybrids from the contact zone between *P. anubis* and *P. cynocephalus* in Amboseli, Kenya exhibit a continuous distribution of phenotypes ranging from more *P. anubis*-like to intermediate to more *P. cynocephalus*-like, while the phenotypic distribution of hybrids in the *P. anubis* x *P. hamadryas* contact zone in Awash, Ethiopia is bimodal with very few intermediate phenotypes (Alberts & Altmann, 2001; Wango et al., 2019). Phenotypically intermediate hybrids in Awash also exhibit reproductive behaviors intermediate to those observed in parental taxa, and are therefore thought to be at a reproductive disadvantage when backcrossing with *P. anubis* or *P. hamadryas* compared to hybrids with predominantly parental phenotypes and behaviors (Bergman et al., 2008). Hybrids in recently formed anthropogenic contact zones show more continuous phenotypic distributions and symmetrical contribution of parental genes into the contact zone (Malukiewicz, 2019). So, a biologically relevant understanding of phenotypic outcomes in hybrid populations requires information regarding a variety of endogenous and exogenous variables.

This study assumes that the NMNH is correct in its taxonomic designations of the specimens used. However, the hybrids and parental taxa studied here have not been genotyped, as is preferable in analyses examining the relationship between phenotype and degree of hybridity (Ackermann et al., 2006; Boel et al., 2019; Cheverud et al., 1993; Hamada et al., 2012). The assumption that the parental taxa are not themselves admixed may be particularly problematic for robust capuchins, as *Sapajus* species have a complex history of hybridization in secondary contact zones (Lima et al., 2018). In addition, there may be cryptic hybrids in the sample with a high degree of genetic admixture but no phenotypic indication of hybridity (Ackermann, 2010; Kelaita & Cortés-Ortiz, 2013). Regardless, the results of the analyses presented here, combined with results from previous research, allow for some predictions to be made regarding the genetic makeup of the robust capuchin hybrids.

My analyses indicate that, while hybrid M^1 shape largely falls within the range of variation observed in *S. nigritus* and *S. libidinosus*, some aspects of hybrid M^1 shape are unique compared to parental morphology. While PC 1 typically captures the allometric component of shape variation (Zelditch et al., 2012), in this study taxonomic designation explained a greater proportion of variation in PC 1 scores than did molar size (Table 2). Hybrids significantly differed from *S. nigritus* and *S. libidinosus* on the main axis of M^1 shape variation in the PCA. Hybrids had significantly lower PC 1 scores than both parental taxa and higher PC 2 scores than *S. libidinosus*, corresponding to M^1s with increased buccolingual distance between cusps and a waisted lingual crown margin (see Figures 3 and 4). However, hybrids and *S. nigritus* did not exhibit significantly different PC 2 or PC 3 scores. So, some hybrids exhibit a unique molar morphotype compared to parents, while others cluster with *S. nigritus*. This was reflected by the reasonably accurate classifications generated by the DFA assignment test (Table 3). *Sapajus nigritus* had the lowest correct assignment (61.3%), with more individuals misclassified as hybrids than *S. libidinosus* (Table 3). *Sapajus libidinosus* specimens also were more often misclassified as hybrids than *S. nigritus* but exhibited the highest percentage of

correctly classified individuals (73.0%).

The results of the PCA and DFA support recent revisions in capuchin taxonomy. Based on genetic and morphological data, the capuchins are proposed to contain two genera: the gracile *Cebus* capuchins and the robust *Sapajus* capuchins (Lynch Alfaro, de Sousa e Silva-Júnior, et al., 2012). The IUCN recognizes eight *Sapajus* species that can be subdivided into a more ancient clade that evolved in the Brazilian Atlantic forest and a clade that recently left the Atlantic Forest to spread throughout the Amazon (Lima et al., 2018). *Sapajus nigritus* belongs to the more ancient clade, and retains morphological features indicative of arboreal living, such as longer limbs and tails. *Sapajus libidinosus* belongs to the Amazonian clade but has recently evolved morphological traits for terrestrial life in the dry shrublands of the Brazilian Cerrado-Caatinga, including thickened molar enamel and shorter, more robust limbs (Wright et al., 2015). *Sapajus libidinosus* is therefore the most morphologically derived robust capuchin species (Wright et al., 2015). The results of the PCA and DFA presented here indicate that *S. nigritus* and *S. libidinosus* exhibit statistically significant differences in M^1 shape. Hybrids cluster more with *S. nigritus* rather than with the more derived *S. libidinosus*. Based on the tendency of the hybrids and *S. nigritus* to cluster along PCs 2 and 3, I would expect the hybrids to exhibit greater genetic affinity with *S. nigritus*. Tail length has been shown to track degree of hybridity in macaques (Hamada et al., 2012), so it would be interesting to test this in *S. nigritus* x *S. libidinosus* hybrids.

Mean hybrid M^1 shape in this study is not the MPV (see Figure 2). Compared to the expected shape, the observed hybrid M^1 mean shape exhibits buccolingual expansion and a waisted lingual margin. However, the MPV is expected only in F1 hybrids and only for traits under additive genetic control (Falconer & Mackay, 1997). It is highly unlikely that wild hybrid populations contain only F1 individuals (Kelaita & Cortés-Ortiz, 2013; Phillips-Conroy & Jolly, 1986). Additionally, it is known that the genetic architecture controlling M^1 size and shape is partly non-additive (Hardin, 2019; Hlusko et al., 2016). Combined, these observations indicate that the deviation from the expected mid-parental M^1 shape observed in this study are likely caused by the disruption of non-additive gene expression or epigenetic interactions in later-generation *S. nigritus* x *S. libidinosus* hybrids. This suggests that the morphological impact of hybridization persists beyond early hybrid generations, as

has been demonstrated in baboons and macaques (Ackermann et al., 2014; Ito et al., 2015).

The *S. nigritus* x *S. libidinosus* hybrids exhibit evidence of destabilized dental development. Measured by pairwise Procrustes distances, hybrids exhibit statistically significant elevation of within-taxon variation in M^1 shape compared to both parental taxa. This variation may be driven by relaxed constraints during dental development (Fuzessy et al., 2014). Indeed, hybrids exhibit lower mean correlation between cusp tip configuration and crown outline shape (*r*-PLS = 0.63) compared to *S. nigritus* and *S. libidinosus* (*r*-PLS = 0.76 and *r*-PLS = 0.75, respectively). Hybrids tend to have wider intercusp distances and cusps positioned closer to the crown periphery than the parental taxa. Cusp tips correspond to the position of embryonic signaling centers in developing tooth germs. The distance between cusp tips is controlled by the relative strengths of activator and inhibitor molecules excreted by each signaling center and the duration of germ growth. Increased inhibitory signaling and/or prolonged germ growth are expected to result in fully formed teeth with widely spaced cusp tips (Guatelli-Steinberg et al., 2013; Jernvall, 2000). So, the wide intercusp distances and weaker correlation of cusp configuration and crown outline shape observed in *S. nigritus* x *S. libidinosus* hybrids are likely the result of prolonged dental development and/or deviation in levels of signaling molecules compared to those observed in parental dental development. Similarly, Ackermann et al. (2014) found that the presence of supernumerary distomolars is associated with increased molar row length in F1 hybrid *P. cynocephalus* x *P. anubis* individuals, suggesting that dental development is prolonged in hybrids compared to parents. Among other papionin hybrids, *Papio hamadryas* x *P. anubis* hybrids exhibit unique molar size relationships compared to parental taxa, suggesting that developmental pathways controlling hybrid baboon molar size may be destabilized compared to unadmixed baboons (Phillips-Conroy, 1978). However, based on frequencies of dental non-metric trait expression and fluctuating asymmetry of bilateral cranial traits, there is no evidence for destabilized dental development in early-generation *M. fuscata* x *M. cyclopis* macaques (Boel et al., 2019). It is possible that these observations support the prediction that the degree of developmental destabilization observed in hybrids is associated with parental divergence. *Sapajus nigritus* and *S. libidinosus* shared a common ancestor around 2.6 Ma (Lima et al., 2018); *P. cynocephalus*

and *P. anubis* diverged approximately 1.5 Ma while *P. hamadryas* and *P. anubis* diverged approximately 800 ka (Rogers et al., 2019); and *M. fuscata* and *M. cyclopis* are estimated to diverge as recently as 170 ka (Chu et al., 2007). A comparison of dental phenotypic variation and integration among these different hybrid populations would confirm the relationship between the degree of parental divergence and destabilized development in hybrids.

While non-metric dental anomalies are observed at high frequencies in some mammalian hybrid populations, this pattern is not shared by all extant primates. This calls into question the suggestion that certain dental non-metric traits, especially supernumerary distomolars or dental crowding, are evidence of significant hybrid ancestry in extinct hominins (Ackermann, 2010; Ackermann et al., 2019). However, continuous dental trait variation remains understudied, even though non-metric dental traits are often correlated with continuous trait variation (Ortiz et al., 2018) and a *Homo sapiens* fossil with substantial *H. neanderthalensis* ancestry exhibits extremely large upper third molars (Fu et al., 2015). The results presented here suggest that transgressive M^1 morphology that falls outside of the range of variation observed in well-defined hominin taxa may be indicative of hybrid ancestry in hominin fossils. Further analyses comparing molar shape variation in other extant primate hybrids would confirm if this is a valid prediction. In terms of primate conservation, this study did not indicate that hybridization reduced phenotypic variation among hybrids of *S. nigritus* and *S. libidinosus*. Rather, hybridization generated novel phenotypes not observed in either parental population. It remains to be determined if expanded intercusp distances in these hybrids facilitate ecological niche separation from other robust capuchin populations.

Conclusions

The dentition has been an anatomical region of interest in hybrid research, but previous work has predominantly studied non-metric dental trait variation rather than tooth shape. The results presented here suggest that a more in-depth analysis of the impact of hybridization on continuous dental phenotypes and development is warranted. The shape of the first upper molar is statistically distinct among *S. nigritus*, *S. libidinosus* and their hybrids, and hybrids exhibit morphological evidence of destabilized development, including elevated within-sample variance and weaker correlation between cusp tip configuration and crown outline shape. The same analyses used here applied to the rest of the postcanine teeth would likely uncover other significant differences between the hybrids and parental taxa. A more comprehensive understanding of the impact of hybridization on dental development could be gained by further comparisons of continuous trait integration between metameres and between occluding upper and lower molars; and by comparing levels of fluctuating asymmetry of continuous traits in left and right antimeres. The data derived from such studies would offer crucial information for attempts to diagnose hybrid ancestry from fossil morphology and to understand the evolutionary outcomes of hybridization among endangered primates in degraded habitats.

REFERENCES

Ackermann, R. R. (2010). Phenotypic traits of primate hybrids: Recognizing admixture in the fossil record. *Evolutionary Anthropology: Issues, News, and Reviews*, *19*(6), 258–270.

Ackermann, R. R., Arnold, M. L., Baiz, M. D., Cahill, J. A., Cortés-Ortiz, L., Evans, B. J., Grant, B. R., Grant, P. R., Hallgrimsson, B., Humphreys, R. A., Jolly, C. J., Malukiewicz, J., Percival, C. J., Ritzman, T. B., Roos, C., Roseman, C. C., Schroeder, L., Smith, F. H., Warren, K. A., … Zinner, D. (2019). Hybridization in human evolution: Insights from other organisms. *Evolutionary Anthropology: Issues, News, and Reviews*, *28*(4), 189–209.

Ackermann, R. R., & Bishop, J. M. (2010). Morphological and molecular evidence reveals recent hybridization between *Gorilla* taxa. *Evolution*, *64*(1), 271–290.

Ackermann, R. R., Brink, J. S., Vrahimis, S., & de Klerk, B. (2010). Hybrid wildebeest (*Artiodactyla*: Bovidae) provide further evidence for shared signatures of admixture in mammalian crania. *South African Journal of Science*, *106*, 1–4.

Ackermann, R. R., Rogers, J., & Cheverud, J. M. (2006). Identifying the morphological signatures of hybridization in primate and human evolution. *Journal of Human Evolution*, *51*(6), 632–645.

Ackermann, R. R., Schroeder, L., Rogers, J., & Che-

verud, J. M. (2014). Further evidence for phenotypic signatures of hybridization in descendant baboon populations. *Journal of Human Evolution*, *76*, 54–62.

Adams, D. C., Collyer, M., & Kaliontzopoulou, A. (2020). *Geomorph: Software for geometric morphometric analyses. R package version 3.2.1*. https://cran.r-project.org/web/packages/geomorph/geomorph.pdf

Adams, D. C., & Collyer, M. L. (2016). On the comparison of the strength of morphological integration across morphometric datasets. *Evolution*, *70*(11), 2623–2631.

Alberts, S. C., & Altmann, J. (2001). Immigration and hybridization patterns of yellow and anubis baboons in and around Amboseli, Kenya. *American Journal of Primatology*, *53*(4), 139–154.

Alibert, P., Renaud, S., Dod, B., Bonhomme, F., & Auffray, J.-C. (1994). Fluctuating asymmetry in the *Mus musculus* hybrid zone: A heterotic effect in disrupted co-adapted genomes. *Proceedings of the Royal Society of London. Series B: Biological Sciences*, *258*(1351), 53–59.

Allen, R., Ryan, H., Davis, B. W., King, C., Frantz, L., Irving-Pease, E., Barnett, R., Linderholm, A., Loog, L., Haile, J., Lebrasseur, O., White, M., Kitchener, A. C., Murphy, W. J., & Larson, G. (2020). A mitochondrial genetic divergence proxy predicts the reproductive compatibility of mammalian hybrids. *Proceedings of the Royal Society B: Biological Sciences*, *287*(1928), 20200690.

Arnold, M. L. (1997). *Natural Hybridization and Evolution*. New York: Oxford University Press, USA.

Arnold, M. L., & Meyer, A. (2006). Natural hybridization in primates: One evolutionary mechanism. *Zoology*, *109*(4), 261–276.

Bailey, S. E. (2002). *Neandertal dental morphology: Implications for modern human origins* [Ph.D. Thesis]. Arizona State University.

Bailey, S. E. (2004). A morphometric analysis of maxillary molar crowns of Middle-Late Pleistocene hominins. *Journal of Human Evolution*, *47*(3), 183–198.

Bailey, S. E., Benazzi, S., Buti, L., & Hublin, J.-J. (2016). Allometry, merism, and tooth shape of the lower second deciduous molar and first permanent molar. *American Journal of Physical Anthropology*, *159*(1), 93–105.

Bergman, T. J., Phillips-Conroy, J. E., & Jolly, C. J. (2008). Behavioral variation and reproductive success of male baboons (*Papio anubis* × *Papio hamadryas*) in a hybrid social group. *American Journal of Primatology*, *70*(2), 136–147.

Bernardes, J. P., Stelkens, R. B., & Greig, D. (2017). Heterosis in hybrids within and between yeast species. *Journal of Evolutionary Biology*, *30*(3), 538–548.

Boel, C. (2016). *The Craniodental Morphology of Hybridising Macaques, and Implications for the Detection of Hybrids in the Human Fossil Record* [Ph.D. Thesis]. University of New South Wales.

Boel, C., Curnoe, D., & Hamada, Y. (2019). Craniofacial Shape and Nonmetric Trait Variation in Hybrids of the Japanese Macaque (*Macaca fuscata*) and the Taiwanese Macaque (*Macaca cyclopis*). *International Journal of Primatology*, *40*, 214–243.

Bolker, B., R Development Core Team, & Giné-Vázquez, I. (2020). *Bbmle* (1.0.23.1) [Computer software].

Bookstein, F. L. (1997). *Morphometric Tools for Landmark Data: Geometry and Biology*. Cambridge: Cambridge University Press.

Browning, S. R., Browning, B. L., Zhou, Y., Tucci, S., & Akey, J. M. (2018). Analysis of Human Sequence Data Reveals Two Pulses of Archaic Denisovan Admixture. *Cell*, *173*(1), 53–61.

Burrell, A. S., Jolly, C. J., Tosi, A. J., & Disotell, T. R. (2009). Mitochondrial evidence for the hybrid origin of the kipunji, *Rungwecebus kipunji* (Primates: Papionini). *Molecular Phylogenetics and Evolution*, *51*(2), 340–348.

Bynum, E. L., Bynum, D. Z., & Supriatna, J. (1997). Confirmation and location of the hybrid zone between wild populations of *Macaca tonkeana* and *Macaca hecki* in Central Sulawesi, Indonesia. *American Journal of Primatology*, *43*(3), 181–209.

Bynum, N. (2002). Morphological variation within a macaque hybrid zone. *American Journal of Physical Anthropology*, *118*(1), 45–49.

Charpentier, M. J. E., Fontaine, M. C., Cherel, E., Renoult, J. P., Jenkins, T., Benoit, L., Barthès, N., Alberts, S. C., & Tung, J. (2012). Genetic structure in a dynamic baboon hybrid zone corroborates behavioural observations in a hybrid population: Population structure in a baboon hybrid zone. *Molecular Ecology*, *21*(3), 715–731.

Charpentier, M. J. E., Tung, J., Altmann, J., & Alberts, S. C. (2008). Age at maturity in wild baboons: Genetic, environmental and demographic influences: Maturation in a hybrid baboon population. *Molecular Ecology*, *17*(8), 2026–2040.

Chen, C., & Pfennig, K. S. (2020). Female toads engaging in adaptive hybridization prefer high-quality heterospecifics as mates. *Science*, *367*(6484), 1377.

Chen, L., Wolf, A. B., Fu, W., Li, L., & Akey, J. M. (2020). Identifying and Interpreting Apparent Neanderthal Ancestry in African Individuals.

Cell, *180*(4), 677–687.

Chen, Z. J. (2013). Genomic and epigenetic insights into the molecular bases of heterosis. *Nature Reviews Genetics*, *14*(7), 471–482.

Cheverud, J. M., Jacobs, S. C., & Moore, A. J. (1993). Genetic differences among subspecies of the saddle-back tamarin (*Saguinus fuscicollis*): Evidence from hybrids. *American Journal of Primatology*, *31*(1), 23–39.

Chhatre, V. E., Evans, L. M., DiFazio, S. P., & Keller, S. R. (2018). Adaptive introgression and maintenance of a trispecies hybrid complex in range-edge populations of Populus. *Molecular Ecology*, *27*(23), 4820–4838.

Chu, J. H., Lin, Y. S., & Wu, H. Y. (2007). Evolution and dispersal of three closely related macaque species, *Macaca mulatta, M. cyclopis*, and *M. fuscata*, in the eastern Asia. *Molecular Phylogenetics and Evolution*, *43*(2), 418–429.

Clarke, G. M. (1993). The genetic basis of developmental stability. I. Relationships between stability, heterozygosity and genomic coadaptation. *Genetica*, *89*(1), 15–23.

Cortés-Ortiz, L., Duda Jr, T. F., Canales-Espinosa, D., García-Orduña, F., Rodríguez-Luna, E., & Bermingham, E. (2007). Hybridization in large-bodied New World primates. *Genetics Society of America*, *176*, 2421–2425.

de Manuel, M., Kuhlwilm, M., Frandsen, P., Sousa, V. C., Desai, T., Prado-Martinez, J., Hernandez-Rodriguez, J., Dupanloup, I., Lao, O., Hallast, P., Schmidt, J. M., Heredia-Genestar, J. M., Benazzo, A., Barbujani, G., Peter, B. M., Kuderna, L. F. K., Casals, F., Angedakin, S., Arandjelovic, M., … Marques-Bonet, T. (2016). Chimpanzee genomic diversity reveals ancient admixture with bonobos. *Science*, *354*(6311), 477–481.

Debat, V., Alibert, P., David, P., Paradis, E., & Auffray Jean-Christophe. (2000). Independence between developmental stability and canalization in the skull of the house mouse. *Proceedings of the Royal Society of London. Series B: Biological Sciences*, *267*(1442), 423–430.

Delgado, M. N., Galbany, J., Górka, K., & Pérez-Pérez, A. (2015). Taxonomic Implications of Molar Morphology Variability in Capuchins. *International Journal of Primatology*, *36*(4), 707–727.

Détroit, F., Mijares, A. S., Corny, J., Daver, G., Zanolli, C., Dizon, E., Robles, E., Grün, R., & Piper, P. J. (2019). A new species of *Homo* from the Late Pleistocene of the Philippines. *Nature*, *568*(7751), 181.

Detwiler, K. M. (2019). Mitochondrial DNA Analyses of *Cercopithecus* Monkeys Reveal a Localized Hybrid Origin for *C. mitis doggetti* in Gombe National Park, Tanzania. *International Journal of Primatology*, *40*(1), 28–52.

Detwiler, K. M., Burrell, A. S., & Jolly, C. J. (2005). Conservation Implications of Hybridization in African Cercopithecine Monkeys. *International Journal of Primatology*, *26*(3), 661–684.

Dobzhansky, T. (1940). Speciation as a Stage in Evolutionary Divergence. *American Society of Naturalists*, *74*(753), 312–321.

Durvasula, A., & Sankararaman, S. (2020). Recovering signals of ghost archaic introgression in African populations. *Science Advances*, *6*(7), eaax5097. https://doi.org/10.1126/sciadv.aax5097

Eichel, K. A., & Ackermann, R. R. (2016). Variation in the nasal cavity of baboon hybrids with implications for late Pleistocene hominins. *Journal of Human Evolution*, *94*, 134–145.

Evans, A. R., Daly, E. S., Catlett, K. K., Paul, K. S., King, S. J., Skinner, M. M., Nesse, H. P., Hublin, J.-J., Townsend, G. C., & Schwartz, G. T. (2016). A simple rule governs the evolution and development of hominin tooth size. *Nature*, *530*(7591), 477–480.

Falconer, D., & Mackay, T. (1997). *Introduction to Quantitative Genetics*. Dover Publications.

Fan, Z., Zhou, A., Osada, N., Yu, J., Jiang, J., Li, P., Du, L., Niu, L., Deng, J., Xu, H., Xing, J., Yue, B., & Li, J. (2018). Ancient hybridization and admixture in macaques (genus *Macaca*) inferred from whole genome sequences. *Molecular Phylogenetics and Evolution*, *127*, 376–386.

Fourie, N. H., Jolly, C. J., Phillips-Conroy, J. E., Brown, J. L., & Bernstein, R. M. (2015). Variation of hair cortisol concentrations among wild populations of two baboon species (*Papio anubis, P. hamadryas*) and a population of their natural hybrids. *Primates*, *56*(3), 259–272.

Fu, Q., Hajdinjak, M., Moldovan, O. T., Constantin, S., Mallick, S., Skoglund, P., Patterson, N., Rohland, N., Lazaridis, I., Nickel, B., Viola, B., Prüfer, K., Meyer, M., Kelso, J., Reich, D., & Pääbo, S. (2015). An early modern human from Romania with a recent Neanderthal ancestor. *Nature*, *524*(7564), 216–219.

Fuzessy, L. F., Silva, I. de O., Malukiewicz, J., Silva, F. F. R., Pônzio, M. do C., Boere, V., & Ackermann, R. R. (2014). Morphological Variation in Wild Marmosets (*Callithrix penicillata* and *C. geoffroyi*) and Their Hybrids. *Evolutionary Biology*, *41*(3), 480–493.

Gamarra, B., Nova Delgado, M., Romero, A., Gal-

bany, J., & Pérez-Pérez, A. (2016). Phylogenetic signal in molar dental shape of extant and fossil catarrhine primates. *Journal of Human Evolution*, *94*, 13–27.

Gligor, M., Ganzhorn, J. U., Rakotondravony, D., Ramilijaona, O. R., Razafimahatratra, E., Zischler, H., & Hapke, A. (2009). Hybridization between mouse lemurs in an ecological transition zone in southern Madagascar. *Molecular Ecology*, *18*(3), 520–533.

Gómez-Robles, A., Bermúdez de Castro, J. M., Martinón-Torres, M., Prado-Simón, L., & Arsuaga, J. L. (2015). A geometric morphometric analysis of hominin lower molars: Evolutionary implications and overview of postcanine dental variation. *Journal of Human Evolution*, *82*, 34–50.

Gómez-Robles, A., Martinón-Torres, M., Bermúdez de Castro, J. M., Margvelashvili, A., Bastir, M., Arsuaga, J. L., Pérez-Pérez, A., Estebaranz, F., & Martínez, L. M. (2007). A geometric morphometric analysis of hominin upper first molar shape. *Journal of Human Evolution*, *53*(3), 272–285.

Goodwin, H. T. (1998). Supernumerary teeth in Pleistocene, recent, and hybrid individuals of the *Spermophilus richardsonii* complex (Sciuridae). *Journal of Mammalogy*, *79*(4), 1161–1169.

Grant, P. R., & Grant, B. R. (2020). Triad hybridization via a conduit species. *Proceedings of the National Academy of Sciences*, *117*(14), 7888–7896.

Green, R. E., Krause, J., Briggs, A. W., Marcic, T., Stenzel, U., Kircher, M., Patterson, N., Li, H., Zhai, W., Fritz, M. H.-Y., Hansen, N. F., Durand, E. Y., Malaspinas, A.-S., Jensen, J. D., Marques-Bonet, T., Alkan, C., Prüfer, kay, Meyer, M., Burbano, H. A., … Siegemund..., M. (2010). A Draft Sequence of the Neandertal Genome. *Science, New Series*, *328*(5979), 710–722.

Grün, R., Pike, A., McDermott, F., Eggins, S., Mortimer, G., Aubert, M., Kinsley, L., Joannes-Boyau, R., Rumsey, M., Denys, C., Brink, J., Clark, T., & Stringer, C. (2020). Dating the skull from Broken Hill, Zambia, and its position in human evolution. *Nature*, *580*, 372–375.

Guatelli-Steinberg, D., Hunter, J. P., Durner, R. M., Moormann, S., Weston, T. C., & Betsinger, T. K. (2013). Teeth, morphogenesis, and levels of variation in the human Carabelli trait. In G. R. Scott & J. D. Irish (Eds.), *Anthropological perspectives on dental morphology: Genetics, evolution, variation.* (pp. 69–91). Cambridge University Press.

Gunz, P., & Mitteroecker, P. (2013). Semilandmarks: A method for quantifying curves and surfaces. *Hystrix, the Italian Journal of Mammalogy*, *24*(1). https://doi.org/10.4404/hystrix-24.1-6292

Hamada, Y., Yamamoto, A., Kunimatsu, Y., Tojima, S., Mouri, T., & Kawamoto, Y. (2012). Variability of tail length in hybrids of the Japanese macaque (*Macaca fuscata*) and the Taiwanese macaque (*Macaca cyclopis*). *Primates*, *53*(4), 397–411. https://doi.org/10.1007/s10329-012-0317-3

Hardin, A. M. (2019). Genetic contributions to dental dimensions in brown-mantled tamarins (*Saguinus fuscicollis*) and rhesus macaques (*Macaca mulatta*). *American Journal of Physical Anthropology*, *168*(2), 292–302.

Heide-Jorgensen, M. P., & Reeves, R. R. (1993). Description of an anomalous monodontid skull from West Greenland: A possible hybrid? *Marine Mammal Science*, *9*(3), 258–268.

Herries, A. I. R., Martin, J. M., Leece, A. B., Adams, J. W., Boschian, G., Joannes-Boyau, R., Edwards, T. R., Mallett, T., Massey, J., Murszewski, A., Neubauer, S., Pickering, R., Strait, D. S., Armstrong, B. J., Baker, S., Caruana, M. V., Denham, T., Hellstrom, J., Moggi-Cecchi, J., … Menter, C. (2020). Contemporaneity of *Australopithecus*, *Paranthropus*, and early *Homo erectus* in South Africa. *Science*, *368*(6486), eaaw7293.

Hlusko, L. J., Schmitt, C. A., Monson, T. A., Brasil, M. F., & Mahaney, M. C. (2016). The integration of quantitative genetics, paleontology, and neontology reveals genetic underpinnings of primate dental evolution. *Proceedings of the National Academy of Sciences*, *113*(33), 9262–9267.

Holliday, T. W. (2003). Species Concepts, Reticulation, and Human Evolution. *Current Anthropology*, *44*(5), 653–673.

Huerta-Sánchez, E., Jin, X., Asan, Bianba, Z., Peter, B. M., Vinckenbosch, N., Liang, Y., Yi, X., He, M., Somel, M., Ni, P., Wang, B., Ou, X., Huasang, Luosang, J., Cuo, Z. X. P., Li, K., Gao, G., Yin, Y., … Nielsen, R. (2014). Altitude adaptation in Tibetans caused by introgression of Denisovan-like DNA. *Nature*, *512*(7513), 194–197.

Ito, T., Kawamoto, Y., Hamada, Y., & Nishimura, T. D. (2015). Maxillary sinus variation in hybrid macaques: Implications for the genetic basis of craniofacial pneumatization. *Biological Journal of the Linnean Society*, *115*(2), 333–347.

Jackson, J. F. (1973). A Search for the Population Asymmetry Parameter. *Systematic Biology*, *22*(2), 166–170.

Jacobs, G. S., Hudjashov, G., Saag, L., Kusuma, P., Darusallam, C. C., Lawson, D. J., Mondal, M., Pagani, L., Ricaut, F.-X., Stoneking, M., Metspa-

lu, M., Sudoyo, H., Lansing, J. S., & Cox, M. P. (2019). Multiple Deeply Divergent Denisovan Ancestries in Papuans. *Cell*, *177*(4), 1010–1021.

Jernvall, J. (2000). Linking development with generation of novelty in mammalian teeth. *Proceedings of the National Academy of Sciences*, *97*(6), 2641–2645.

Jernvall, J., & Jung, H.-S. (2000). Genotype, phenotype, and developmental biology of molar tooth characters. *American Journal of Physical Anthropology*, *113*(s 31), 171–190.

Jiggins, C. D., Salazar, C., Linares, M., & Mavarez, J. (2008). Hybrid trait speciation and Heliconius butterflies. *Philosophical Transactions of the Royal Society B: Biological Sciences*, *363*(1506), 3047–3054.

Jolly, C. J., Burrell, A. S., Phillips-Conroy, J., E., Bergey, C., & Rogers, J. (2011). Kinda baboons (*Papio kindae*) and grayfoot chacma baboons (*P. ursinus griseipes*) hybridize in the Kafue river valley, Zambia. *American Journal of Primatology*, *73*(3), 291–303.

Jolly, C. J., Woolley-Barker, T., Beyene, S., Disotell, T. R., & Phillips-Conroy, J. E. (1997). Intergeneric Hybrid Baboons. *International Journal of Primatology*, *18*(4), 597–627.

Kavanagh, K. D., Evans, A. R., & Jernvall, J. (2007). Predicting evolutionary patterns of mammalian teeth from development. *Nature*, *449*(7161), 427–432.

Kelaita, M. A., & Cortés-Ortiz, L. (2013). Morphological variation of genetically confirmed *Alouatta Pigra* × *A. palliata* hybrids from a natural hybrid zone in Tabasco, Mexico. *American Journal of Physical Anthropology*, *150*(2), 223–234.

Klingenberg, C. P. (2003). Developmental instability as a research tool: Using patterns of fluctuating asymmetry to infer the developmental origins of morphological integration. In M. Polak (Ed.), *Developmental Instability: Causes and Consequences* (pp. 427–442). Oxford University Press.

Klingenberg, C. P., & McIntyre, G. S. (1998). Geometric Morphometrics of Developmental Instability: Analyzing Patterns of Fluctuating Asymmetry with Procrustes Methods. *Evolution*, *52*(5), 1363–1375.

Kohn, L. A. P., Langton, L. B., & Cheverud, J. M. (2001). Subspecific genetic differences in the saddle-back tamarin (*Saguinus fuscicollis*) postcranial skeleton. *American Journal of Primatology*, *54*(1), 41–56.

Kuhlwilm, M., Han, S., Sousa, V. C., Excoffier, L., & Marques-Bonet, T. (2019). Ancient admixture from an extinct ape lineage into bonobos. *Nature*

Ecology & Evolution.

Leary, R. F., Allendorf, F. W., & Knudsen, K. L. (1985). Developmental instability and high meristic counts in interspecific hybrids of salmonid fishes. *Evolution*, *39*(6), 1318–1326.

Lima, M. G. M., de Sousa e Silva-Júnior, J., Černý, D., Buckner, J. C., Aleixo, A., Chang, J., Zheng, J., Alfaro, M. E., Martins, A., Di Fiore, A., Boubli, J. P., & Lynch Alfaro, J. W. (2018). A phylogenomic perspective on the robust capuchin monkey (*Sapajus*) radiation: First evidence for extensive population admixture across South America. *Molecular Phylogenetics and Evolution*, *124*, 137–150.

Lynch Alfaro, J. W., Boubli, J. P., Olson, L. E., Di Fiore, A., Wilson, B., Gutiérrez-Espeleta, G. A., Chiou, K. L., Schulte, M., Neitzel, S., Ross, V., Schwochow, D., Nguyen, M. T. T., Farias, I., Janson, C. H., & Alfaro, M. E. (2012). Explosive Pleistocene range expansion leads to widespread Amazonian sympatry between robust and gracile capuchin monkeys. *Journal of Biogeography*, *39*(2), 272–288.

Lynch Alfaro, J. W., de Sousa e Silva-Júnior, J., & Rylands, A. B. (2012). How Different Are Robust and Gracile Capuchin Monkeys? An Argument for the Use of *Sapajus* and *Cebus*. *American Journal of Primatology*, *74*(4), 273–286.

Lynch Alfaro, J. W., Izar, P., & Ferreira, R. G. (2014). Capuchin monkey research priorities and urgent issues. *American Journal of Primatology*, *76*(8), 705–720.

Malukiewicz, J. (2019). A Review of Experimental, Natural, and Anthropogenic Hybridization in *Callithrix* Marmosets. *International Journal of Primatology*, *40*, 72–98.

Malukiewicz, J., Boere, V., Fuzessy, L. F., Grativol, A. D., de Oliveira e Silva, I., Pereira, L. C. M., Ruiz-Miranda, C. R., Valença, Y. M., & Stone, A. C. (2015). Natural and Anthropogenic Hybridization in Two Species of Eastern Brazilian Marmosets (*Callithrix jacchus* and *C. penicillata*). *PLOS ONE, 10*(6), e0127268.

Martinón-Torres, M., Bermúdez de Castro, J. M., Gómez-Robles, A., Prado-Simón, L., & Arsuaga, J. L. (2012). Morphological description and comparison of the dental remains from Atapuerca-Sima de los Huesos site (Spain). *Journal of Human Evolution*, *62*(1), 7–58.

Martins, W. P., Lynch Alfaro, J., & Rylands, A. B. (2017). Reduced range of the endangered crested capuchin monkey (*Sapajus robustus*) and a possible hybrid zone with *Sapajus nigritus*. *American Journal of Primatology*, *79*(10), e22696.

Mather, R. (1992). *A field study of hybrid gibbons in central Kalimantan, Indonesia* [Ph.D. Thesis]. University of Cambridge.

Mayr, E. (1963). *Animal species and evolution.* The Belknap Press of Harvard University Press.

Melo, F. R., Alfaro, J. L., Miranda, J. M. D., Rímoli, J., Alonso, A. C., Santos, M. C. dos, Ludwig, G., Martins, W. P., & Martins, J. N. (2015, January 26). *IUCN Red List of Threatened Species: Black-horned Capuchin*. IUCN Red List of Threatened Species. https://www.iucnredlist.org/en

Melo, F. R., Fialho, M. de S., Jerusalinsky, L., Laroque, P. de O., Alfaro, J. L., Montenegro, M. M. V., Bezerra, B. M., & Martins, A. B. (2015, January 26). *IUCN Red List of Threatened Species: Bearded Capuchin*. IUCN Red List of Threatened Species. https://www.iucnredlist.org/en

Mourthe, I., Trindade, R. A., Aguiar, L. M., Trigo, T. C., Bicca-Marques, J. C., & Bonatto, S. L. (2019). Hybridization Between Neotropical Primates with Contrasting Sexual Dichromatism. *International Journal of Primatology*, *40*(1), 99–113.

Neff, N. A., & Smith, G. R. (1979). Multivariate Analysis of Hybrid Fishes. *Systematic Zoology*, *28*(2), 176–196.

Ortiz, A., Bailey, S. E., Schwartz, G. T., Hublin, J.-J., & Skinner, M. M. (2018). Evo-devo models of tooth development and the origin of hominoid molar diversity. *Science Advances*, *4*(4), eaar2334. https://doi.org/10.1126/sciadv.aar2334

Pallares, L. F., Turner, L. M., & Tautz, D. (2016). Craniofacial shape transition across the house mouse hybrid zone: Implications for the genetic architecture and evolution of between-species differences. *Development Genes and Evolution*, *226*(3), 173–186.

Paul, K. S., Astorino, C. M., & Bailey, S. E. (2017). The Patterning Cascade Model and Carabelli's trait expression in metameres of the mixed human dentition: Exploring a morphogenetic model. *American Journal of Physical Anthropology*, *162*(1), 3–18.

Phillips-Conroy, J. E. (1978). *Dental Variability in Ethiopian Baboons: An Examination of the Anubis-Hamadryas Hybrid Zone in the Awash National Park, Ethiopia* [Ph.D. Thesis]. New York University.

Phillips-Conroy, J. E., & Jolly, C. J. (1986). Changes in the structure of the baboon hybrid zone in the Awash National Park, Ethiopia. *American Journal of Physical Anthropology*, *71*(3), 337–350.

Reich, D., Patterson, N., Kircher, M., Delfin, F.,

Nandineni, M. R., Pugach, I., Ko, A. M.-S., Ko, Y.-C., Jinam, T. A., Phipps, M. E., Saitou, N., Wollstein, A., Kayser, M., Pääbo, S., & Stoneking, M. (2011). Denisova Admixture and the First Modern Human Dispersals into Southeast Asia and Oceania. *The American Journal of Human Genetics*, *89*(4), 516–528. https://doi.org/10.1016/j.ajhg.2011.09.005

Rizk, O. T., Grieco, T. M., Holmes, M. W., & Hlusko, L. J. (2013). Using geometric morphometrics to study the mechanisms that pattern primate dental variation. *Anthropological Perspectives on Tooth Morphologies: Genetics, Evolution, Variation. Cambridge: Cambridge University Press. p*, 126–169.

Rogers, J., Raveendran, M., Harris, R. A., Mailund, T., Leppälä, K., Athanasiadis, G., Schierup, M. H., Cheng, J., Munch, K., Walker, J. A., Konkel, M. K., Jordan, V., Steely, C. J., Beckstrom, T. O., Bergey, C., Burrell, A., Schrempf, D., Noll, A., Kothe, M., … Baboon Genome Analysis Consortium. (2019). The comparative genomics and complex population history of *Papio* baboons. *Science Advances*, *5*(1), eaau6947. https://doi.org/10.1126/sciadv.aau6947

Roos, C., Liedigk, R., Thinh, V. N., Nadler, T., & Zinner, D. (2019). The Hybrid Origin of the Indochinese Gray Langur *Trachypithecus crepusculus* . *International Journal of Primatology*, *40*(1), 9–27.

Sankararaman, S., Mallick, S., Patterson, N., & Reich, D. (2016). The combined landscape of Denisovan and Neanderthal ancestry in present-day humans. *Current Biology*, *26*(9), 1241–1247.

Seehausen, O., Takimoto, G., Roy, D., & Jokela, J. (2008). Speciation reversal and biodiversity dynamics with hybridization in changing environments. *Molecular Ecology*, *17*(1), 30–44. https://doi.org/10.1111/j.1365-294X.2007.03529.x

Skov, L., Coll Macià, M., Sveinbjörnsson, G., Mafessoni, F., Lucotte, E. A., Einarsdóttir, M. S., Jonsson, H., Halldorsson, B., Gudbjartsson, D. F., Helgason, A., Schierup, M. H., & Stefansson, K. (2020). The nature of Neanderthal introgression revealed by 27,566 Icelandic genomes. *Nature*. https://doi.org/10.1038/s41586-020-2225-9

Slon, V., Mafessoni, F., Vernot, B., de Filippo, C., Grote, S., Viola, B., Hajdinjak, M., Peyrégne, S., Nagel, S., Brown, S., Douka, K., Higham, T., Kozlikin, M. B., Shunkov, M. V., Derevianko, A. P., Kelso, J., Meyer, M., Prüfer, K., & Pääbo, S.

(2018). The genome of the offspring of a Neanderthal mother and a Denisovan father. *Nature*, *561*(7721), 113–116.

Spoor, F., Gunz, P., Neubauer, S., Stelzer, S., Scott, N., Kwekason, A., & Dean, M. C. (2015). Reconstructed *Homo habilis* type OH 7 suggests deep-rooted species diversity in early *Homo*. *Nature*, *519*(7541), 83–86.

Stelkens, R., & Seehausen, O. (2009). Genetic Distance Between Species Predicts Novel Trait Expression in Their Hybrids. *Evolution*, *63*(4), 884–897.

Svardal, H., Jasinska, A. J., Apetrei, C., Coppola, G., Huang, Y., Schmitt, C. A., Jacquelin, B., Ramensky, V., Müller-Trutwin, M., Antonio, M., Weinstock, G., Grobler, J. P., Dewar, K., Wilson, R. K., Turner, T. R., Warren, W. C., Freimer, N. B., & Nordborg, M. (2017). Ancient hybridization and strong adaptation to viruses across African vervet monkey populations. *Nature Genetics*, *49*(12), 1705–1713.

Taylor, S. A., & Larson, E. L. (2019). Insights from genomes into the evolutionary importance and prevalence of hybridization in nature. *Nature Ecology & Evolution*, *3*(2), 170–177.

The GIMP Development Team. (2019). *GNU Image Manipulation Program* (2.10.12) [Computer software]. www.gimp.org

Thinh, V. N., Mootnick, A. R., Geissmann, T., Li, M., Ziegler, T., Agil, M., Moisson, P., Nadler, T., Walter, L., & Roos, C. (2010). Mitochondrial evidence for multiple radiations in the evolutionary history of small apes. *BMC Evolutionary Biology*, *10*(1), 74.

Thompson, K. A., Rieseberg, L. H., & Schluter, D. (2018). Speciation and the City. *Trends in Ecology & Evolution*, *33*(11), 815–826.

Tosi, A. J., Morales, J. C., & Melnick, D. J. (2000). Comparison of Y Chromosome and mtDNA Phylogenies Leads to Unique Inferences of Macaque Evolutionary History. *Molecular Phylogenetics and Evolution*, *17*(2), 133–144.

Tung, J., & Barreiro, L. B. (2017). The contribution of admixture to primate evolution. *Current Opinion in Genetics & Development*, *47*, 61–68.

Villanea, F. A., & Schraiber, J. G. (2019). Multiple episodes of interbreeding between Neanderthal and modern humans. *Nature Ecology & Evolution*, *3*(1), 39–44.

Wang, B., Zhou, X., Shi, F., Liu, Z., Roos, C., Garber, P. A., Li, M., & Pan, H. (2015). Full-length *Numt* analysis provides evidence for hybridization between the Asian colobine genera *Trachypithecus* and *Semnopithecus*: A *Numt* Clarifies a Colobine Hybridization Event. *American Journal of Primatology*, *77*(8), 901–910.

Wango, T. L., Musiega, D., Mundia, C. N., Altmann, J., Alberts, S. C., & Tung, J. (2019). Climate and Land Cover Analysis Suggest No Strong Ecological Barriers to Gene Flow in a Natural Baboon Hybrid Zone. *International Journal of Primatology*, *40*(1), 53–70.

Wood, B. A., & Abbott, S. A. (1983). Analysis of the dental morphology of Plio-Pleistocene hominids. I. Mandibular molars: Crown area measurements and morphological traits. *Journal of Anatomy*, *136*(Pt 1), 197–219. PubMed.

Wright, K. A., Wright, B. W., Ford, S. M., Fragaszy, D., Izar, P., Norconk, M., Masterson, T., Hobbs, D. G., Alfaro, M. E., & Lynch Alfaro, J. W. (2015). The effects of ecology and evolutionary history on robust capuchin morphological diversity. *Molecular Phylogenetics and Evolution*, *82*, 455–466.

Zelditch, M. L., Swiderski, D. L., & Sheets, H. D. (2012). *Geometric Morphometrics for Biologists: A Primer*. Amsterdam: Elsevier.

Zichello, J. M. (2018). Look in the trees: Hylobatids as evolutionary models for extinct hominins. *Evolutionary Anthropology: Issues, News, and Reviews*, *27*(4), 142–146.

Zinner, D., Arnold, M. L., & Roos, C. (2011). The strange blood: Natural hybridization in primates. *Evolutionary Anthropology: Issues, News, and Reviews*, *20*(3), 96–103.